Improvement of resonant laser ablation mass spectrometry using high-repetition-rate and short-pulse tunable laser system

Watanabe, Kenichi
Department of Nuclear Engineering, Graduate School of Engineering, Nagoya University

Hattori, Kazuhiro
Department of Nuclear Engineering, Graduate School of Engineering, Nagoya University

Kawarabayashi, Jun
Department of Nuclear Engineering, Graduate School of Engineering, Nagoya University

Iguchi, Tetsuo
Department of Nuclear Engineering, Graduate School of Engineering, Nagoya University

https://hdl.handle.net/2324/7168369

出版情報：Spectrochimica Acta Part B: Atomic Spectroscopy. 58 (6), pp.1163-1169, 2003-06-30. Elsevier
バージョン：
権利関係：

Improvement of Resonant Laser Ablation Mass Spectrometry Using High-Repetition-Rate and Short-Pulse Tunable Laser System

Kenichi Watanabe, Kazuhiro Hattori and Tetsuo Iguchi

Department of Nuclear Engineering, Graduate School of Engineering, Nagoya University

Furo-cho, Chikusa-ku, Nagoya 464-8603, Japan

Abstract

The mass spectrometry based on Resonant Laser Ablation technique (RLA-MS), which combines Laser Ablation (LA) and Resonance Ionization Spectroscopy (RIS) simultaneously with a single laser, can be used as a simple analytical technique of trace elements with high sensitivity and elemental (isotopic) selectivity for solid samples. In this study, a high-repetition-rate and short-pulse tunable laser (Ti:Sapphire laser) system is applied to improve the performance of RLA-MS. The basic performance has been checked through experiments and theoretical calculations for trace aluminum(Al) detection. The results show that the present RLA-MS system has a detection limit concentration around 3 ppb/s for Al, which would be about 100 times better than that of the conventional relatively low-repetition-rate and long-pulse dye laser system. The effectiveness of applying a short-pulse laser to RLA-MS is also discussed from the viewpoint of shortening an expansion time of the ablated vapor, which might lead to an advantage of the system compactness.

KEYWORDS: resonance ionization mass spectrometry, resonant laser ablation, high-repetition-rate and short-pulse tunable laser, neutron dosimetry, detection limit concentration

1. Introduction

The Resonant Laser Ablation (RLA) technique combines Laser Ablation (LA) and Resonance Ionization Spectroscopy (RIS) simultaneously with a single laser. The mass spectrometry based on RLA (Resonant Laser Ablation Mass Spectrometry: RLA-MS) can be used as a simple analytical technique of trace elements with high sensitivity and elemental (isotopic) selectivity for solid samples[1-4]. When the laser output is split into two beams for LA and RIS, in this technique (named the laser beam split RLA), the laser power can be separately controlled for LA and RIS to suppress non-resonance ionization on LA and also to increase the resonance ionization efficiency. In addition, the RIS laser can ionize the ablated vapor effectively because the RIS effective ionization area is as close to the LA spot as possible.

We are now trying to apply this RLA-MS to the detection of trace long-lived radionuclides and/or stable nuclides produced through nuclear reactions between neutrons and nuclear reactor materials, which would lead to a new neutron dosimetry technique as an alternative of the conventional activation analysis. Other techniques for mass spectrometry, such as Inductively Coupled Plasma Mass Spectrometry (ICP-MS) and Accelerator Mass Spectrometry (AMS), are also promising candidates for this application, but they suffer from isobaric interference, which can be easily avoided in RLA-MS.

As a demonstration of the detection of trace long-lived radionuclides, we are attempting the detection of ^{26}Al ($T_{1/2}$: 7.2×10^{5} y) produced by ^{27}Al(n,2n) reaction in high energy neutron fields[5]. Al alloys and ceramics are promising low-activation materials for fusion reactors and/or high energy accelerators. The determination of trace long-lived radionuclides produced in Al material due to high energy neutrons is quite important from the viewpoint of reduction of the radioactive waste. It is, however, difficult to detect ^{26}Al with conventional activation analysis because of its extremely long half-life. The direct detection techniques without the elemental selectivity are affected by the isobaric interference of ^{26}Mg contained in the Al material as an impurity.

So far, we were able to obtain the detection limit concentration of a few ppm per one laser shot for Al, which is contained as an impurity in some alloy materials[6]. The detection limit concentration can be improved if the number of detected ions of interest can be increased, which means that a large number of laser shots are needed. Therefore, to improve the detection limit concentration per unit time, it is effective that the repetition rate of a laser shot should be increased. On the other hand, a high-repetition-rate laser system has generally low power. To vaporize a solid sample with a low power laser, it is necessary that the laser pulse duration should be short and the laser power density should be high.

In this study, we propose the RLA-MS system using high-repetition-rate and short-pulse tunable laser system, and discuss its applicability through basic experiments and theoretical calculations by comparing the basic performance between the present RLA-MS system and the conventional system with a relatively low-repetition-rate and long-pulse tunable laser. Here our present RLA-MS system uses a 1 kHz and 100 ps Ti:Sapphire laser, while the conventional one uses a 10 Hz and 10 ns dye laser.

2. Experimental setup

Figure 1 shows a schematic of our experimental system, which consists of an all solid-state high-repetition-rate and short-pulse tunable Ti:Sapphire laser system with a regenerative amplifier and a reflectron TOF mass spectrometer with a field-free drift region approximately 150 cm long and a microchannel plate

(MCP) ion detector. The mass resolution ($m/\Delta m$) of this reflectron TOF mass spectrometer is approximately 200. This Ti:Sapphire regenerative amplifier system (Spectra-Physics, Spitfire) is designed to amplify single pulses from a mode-locked Ti:Sapphire laser (Spectra-Physics, Tsunami) as the optical pulse passes through a Ti:Sapphire laser rod, which has been optically excited by a laser pulse from a Nd:YLF laser (Spectra-Physics, Evolution). The output from this amplifier is frequency doubled using a second harmonic generation crystal (KDP crystal). The bandwidth of the laser was 0.4 cm^{-1}, the laser pulse duration 100 ps and the repetition rate 1 kHz, respectively. This Ti:Sapphire laser system has normally an ultra-short pulse duration (100fs-2ps), but our system is customized to a long pulse version (>100ps) to suppress the non-resonance ionization process (i.e. to keep elemental selectivity). On the other hand, the conventional RLA-MS system used the tunable dye laser pumped by a pulsed Nd: YAG laser. This dye laser had the bandwidth of 0.14 cm^{-1}, the laser pulse duration of 10 ns, the repetition rate of 10 Hz and the typical laser output energy of 5 mJ/pulse. The laser output is split into two beams for LA and RIS because the laser power can be separately controlled for LA and RIS to suppress non-resonance ionization on LA and to increase resonance ionization efficiency. The RIS laser pulse was delayed to the LA laser one for 65 ns, corresponding to a finite time for expansion of the atoms vaporized by LA. In this arrangement, the RIS laser can ionize the ablated vapor effectively because the RIS effective ionization area was as close to the LA spot as possible. The laser beams were focused at an ionization area with a diameter of 50 μm. The tunable wavelength range is 450-475nm. The typical laser output energy was 50 μJ/pulse (2.5×10^{10} W/cm^2) for RIS and 2 μJ/pulse (1×10^9 W/cm^2) for LA, respectively.

As the preliminary experiments to confirm the RLA phenomena, copper contained as an impurity in a stainless steel rod was analyzed under a single beam RLA, where the single laser beam with the resonance wavelength for the element of interest is used as LA and RIS lasers simultaneously. As the resonance ionization scheme, two-photon excitation followed by one photon ionization at the same wavelength, that is, the “2+1” transition was adopted because it is quite simple and suitable for one tunable laser. The laser wavelength was tuned to 463.637 nm corresponding to the two photons resonance excitation from $3d^{10}4s$ $^2S_{1/2}$ to $3d^{10}5s$ $^2S_{1/2}$ for copper.

In the experiments to check the basic performance of the present RLA-MS, Al contained in kovar (Ni: 29 %, Co: 17 %, Mg: 0.1 %, Al: 0.1 %, Fe: Balance) alloy rod was analyzed under the laser beam split RLA. The laser wavelength was tuned to 457.467 nm corresponding to the two photons resonance excitation from $3s^23p$ $^2P^o_{1/2,3/2}$ to $3s^25f$ $^2F^o_{5/2,7/2}$ for Al. The detection limit concentration and the elemental selectivity of Al to Mg was estimated for ^{26}Al detection.

3. Outline of theoretical model

We have developed the theoretical model to simulate elementary processes during RLA. This theoretical model couples the vaporization and ionization process on the sample surface[7]. In the vaporization process of this model, the particle flux balance is calculated between the vapor and solid phases of sample materials through the ablated sample surface. We can define the net number of vaporized particles through the ablated sample surface, $f_{net}(T_s, N_v)$, as follows:

$$f_{net}(T_s,N_v) = f_{out}(T_s) - f_{in}(T_s,N_v), \qquad (1)$$

where $f_{out}(T_s)$ and $f_{in}(T_s, N_v)$ are the particle fluxes emitted out from and flowed into the sample surface, respectively, as a function of T_s; the temperature of the sample surface and N_v; the vapor density near the sample surface. The T_s can be obtained by solving the equation of heat conduction, while the N_v can be determined from the motion of vapor through the equations for gas dynamics.

The ionization probability in the net particle flux consists of two components from resonant and non-resonant (or thermal) ionization processes.

4. Results and discussion

In the preliminary experiments, the fundamental phenomena on RLA with a high-repetition-rate and short-pulse tunable Ti:Sapphire laser system were confirmed by analyzing copper contained as an impurity in a stainless steel rod under the single beam RLA. Figure 2 shows the TOF mass spectrum under the single beam RLA at the resonant and non-resonant wavelength for copper. The peak area of each isotope corresponds to its ion yield and can be convert to the number of ions by dividing by the peak area for one ion. It is found that only the copper peaks are enhanced at the resonant wavelength. The wavelength dependence of the ion yield under the single beam RLA at the laser power of 5.9×10^8 and 8.6×10^8 W/cm^2 is shown in Fig .3, where the peak at 463.637 nm is clearly observed, corresponding to the two photons resonant transition from $3d^{10}4s\ ^2S_{1/2}$ to $3d^{10}5s\ ^2S_{1/2}$ for copper. The FWHM of this peak is 0.014 nm(0.47 cm^{-1}) and is corresponding to the bandwidth of the Ti:Sapphire laser(0.4 cm^{-1}) rather than the natural resonance width.

In the performance verification experiments for the present RLA-MS system, Al contained in a kovar alloy rod was analyzed under the laser beam split RLA. Figure 4 gives the TOF mass spectra, where the split two beams for LA and RIS and only one beam for LA are used at the resonant wavelength of Al. It is found that the Al ion yield is enhanced by using the RIS laser. To estimate the elemental selectivity and the detection limit concentration under the laser beam split RLA, the LA laser power dependence of Al and Mg ion yields is shown in Fig. 5, which gives the fundamental performances on the detection of trace element with isobaric interference. The dots and lines in Fig.5 are the experimental and calculated data, respectively. In the theoretical model calculation, for the ionization process, only the thermal ionization process on LA is considered for Mg and both of the thermal and resonance ionization processes are considered for Al. The experimental and calculated results show good agreement. In high LA laser power region, the ion yield for Mg increases by the thermal ionization process on LA and the elemental selectivity for Al deteriorates. The elemental selectivity of Al to Mg is defined as the ratio of the ion yield of Al to that of Mg. The detection limit concentration for Al is the concentration that can be detected as one ion at least with a MCP ion detector. Therefore, the detection limit concentration C_{limit} can be given as the following simple equation:

$$C_{limit} = \frac{C_{int}}{N_{detect}} \qquad (2)$$

where C_{int} is the concentration of an element of interest (Al) in a sample and N_{detect} is the number of detected ions in that sample. The LA laser power dependence of the elemental selectivity and the detection limit concentration for the present Ti:Sapphire laser system and the conventional dye laser system are summarized in Figs. 6 and 7, respectively[5]. It is found that the detection limit concentrations per one laser shot are 3ppm for both the present Ti:Sapphire laser and the conventional dye laser systems at the laser power with the elemental selectivity of 10^{-3}. Here the elemental selectivity of 10^{-3} has been assumed under the condition that the ^{26}Al of 1 ppb concentration, which can be produced by irradiation of 14 MeV neutron fluence of 10^{17} n/cm^{2} to high purity Al, should be detected in a sample generally containing the ^{26}Mg impurity of 1 ppm concentration[6]. The detection limit concentrations per unit time for the present laser system (1 kHz) and the conventional laser system (10 Hz) are 3 ppb/s and 300 ppb/s, respectively. It has been, therefore, demonstrated that the detection limit concentration would be improved about 100 times by using the high-repetition-rate and short-pulse Ti:Sapphire laser system instead of the conventional relatively low-repetition-rate and long-pulse dye laser system.

As another effectiveness of applying a short-pulse laser to RLA-MS, we have noticed expansion time of the ablated vapor. The theoretical calculation was made on the time spent for expansion of the ablated vapor from a sample surface to the RIS laser spot with the distance of 50 μm. Figure 8 shows the laser power dependence of the expansion time for the short-pulse (100 ps) laser system and the conventional long-pulse (10 ns) laser system. From Fig. 8, the expansion time with the short-pulse laser is found less than that with the long-pulse laser. It is considered that the vapor rapidly ablated by a short-pulse laser has a large driving force for expansion due to its high concentration gradient. The short expansion time, therefore, can shorten the delay time of the RIS laser to the LA laser, which might have an advantage to make a compact system because the light path of the RIS laser to control the delay time to the LA laser can be short.

5. Conclusions

In this study, we have applied a high-repetition-rate (1 kHz) and short-pulse (100 ps) tunable Ti:Sapphire laser system to RLA-MS instead of the conventional relatively low-repetition-rate (10 Hz) and long-pulse (10 ns) dye laser system to improve the detection limit concentration, keeping elemental selectivity. Through the experiments and theoretical calculation to check the basic performance, we have demonstrated that the present RLA-MS system has a detection limit concentration around 3 ppb/s for Al, which would be about 100 times better than that of the conventional relatively low-repetition-rate and long-pulse dye laser system. In addition, it has been pointed out that the light path of the RIS laser for the delay time to the LA laser can be short by using a short-pulse laser system, which might lead to an advantage of the system compactness.

Acknowledgements

The present study is supported by the JAERI's Nuclear Research Promotion Program (JANP).

References

[1] L. Wang, I. S. Borthwick, R. Jennings, P. T. McCombes, K. W. D. Ledingham, R. P. Singhal and C. J. McLean, The Detailed Characteristics of Resonant Laser Ablation, Inst. Phys. Conf. Ser. 114 (1991) 455-458.

[2] L. Wang, I. S. Borthwick, R. Jennings, P. T. McCombes, K. W. D. Ledingham, R. P. Singhal and C. J. McLean, Observations and Analysis of Resonant Laser Ablation of GaAs, Appl. Phys. B 53 (1991) 455-458.

[3] G. C. Eiden, J. E. Anderson and N. S. Nogar, Resonant Laser Ablation: Semiquantitative Aspects and Threshold Effects, Microchem. J. 50 (1994) 289-300.

[4] C. G. Gill, A. W. Garrett, P. H. Hemberger and N. S. Nogar, Selective Laser Ablation/Ionization for Ion Trap Mass Spectrometry: Resonant Laser Ablation, Spectrochim. Acta B 51 (1996) 851-862.

[5] K. Watanabe and T. Iguchi, Trace Element Analysis Using Resonant Laser Ablation, J. Nucl. Sci. Technol. 39 (2002) 312-315.

[6] K. Watanabe and T. Iguchi, Optimization of Trace Element Analysis using Resonant Laser Ablation, AIP Conf. Proc. 584 (2001) 135-140.

[7] K. Watanabe and T. Iguchi, Modeling of Vaporization Processes of Resonant Laser Ablation, Appl. Phys. A 69 (1999) S845-S848.

FIGURE CAPTIONS

Fig. 1 Schematic of our RLA-MS system.

Fig. 2 TOF mass spectrum under the single beam RLA at the resonant and non-resonant wavelength for copper.

Fig. 3 Wavelength dependence of the Cu ion yield under the single beam RLA.

Fig. 4 TOF mass spectra, where the split two beams for LA and RIS and only one beam for LA are used at the resonant wavelength of Al.

Fig. 5 Laser power dependence of Al and Mg ion yields. Dots: experimental results. Lines: calculated results.

Fig. 6 LA laser power dependence of the elemental selectivity and the detection limit concentration for the present Ti:Sapphire laser system. Dots: experimental results. Lines: calculated results.

Fig. 7 LA laser power dependence of the elemental selectivity and the detection limit concentration for the conventional dye laser system. Dots: experimental results. Lines: calculated results.

Fig. 8 Laser power dependence of expansion time of the ablated vapor.

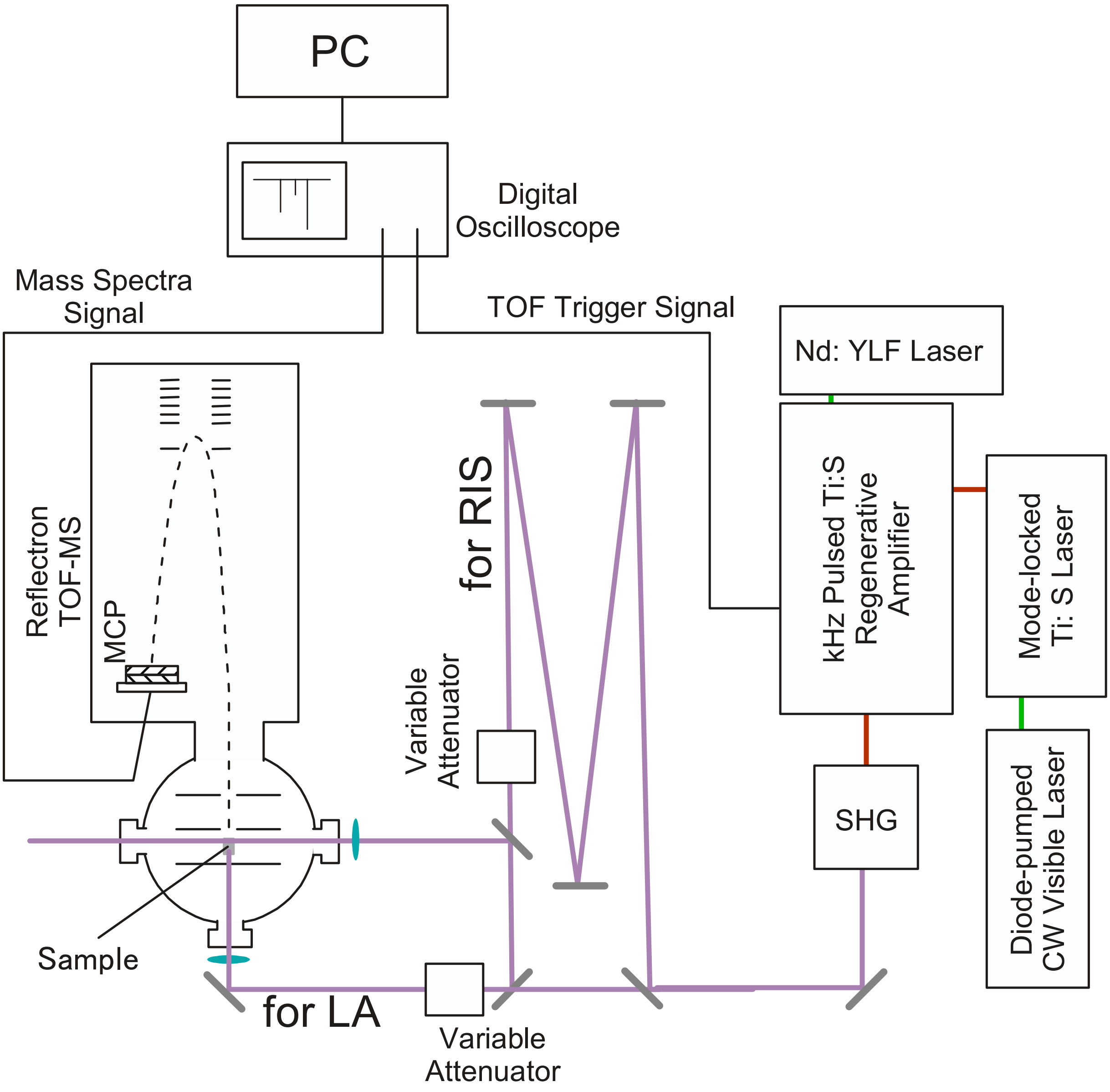

Fig. 1 K. Watanabe et al.

"Improvement of Resonant Laser Mass Spectrometry Using High-Repetition-Rate and Short-Pulse Tunable Laser System "

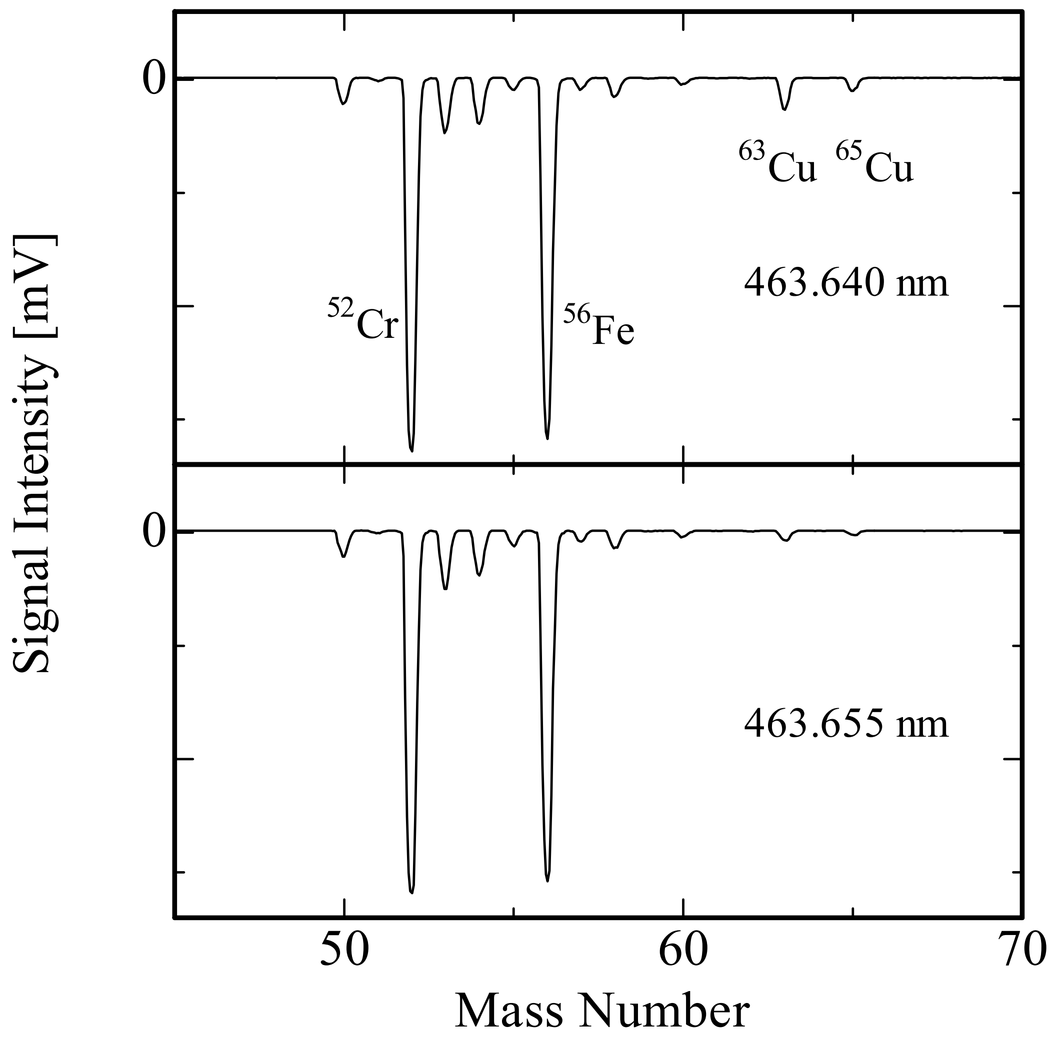

Fig. 2 K. Watanabe et al.

"Improvement of Resonant Laser Mass Spectrometry Using High-Repetition-Rate and Short-Pulse Tunable Laser System "

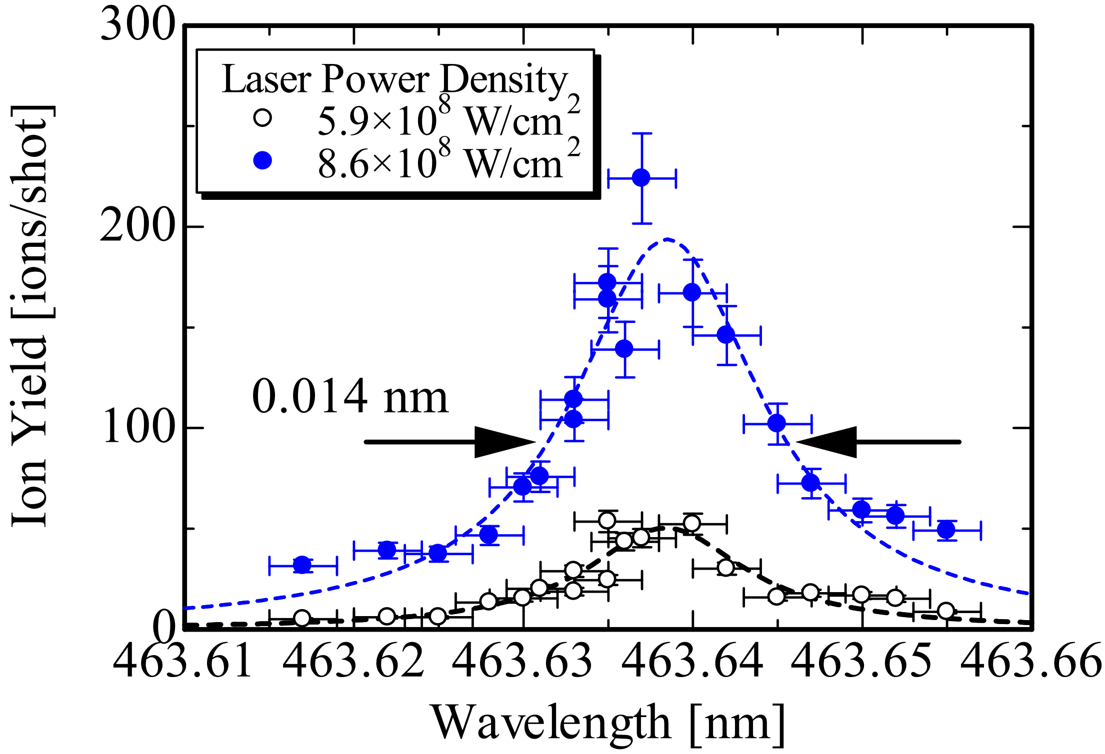

Fig. 3 K. Watanabe et al.

"Improvement of Resonant Laser Mass Spectrometry Using High-Repetition-Rate and Short-Pulse Tunable Laser System "

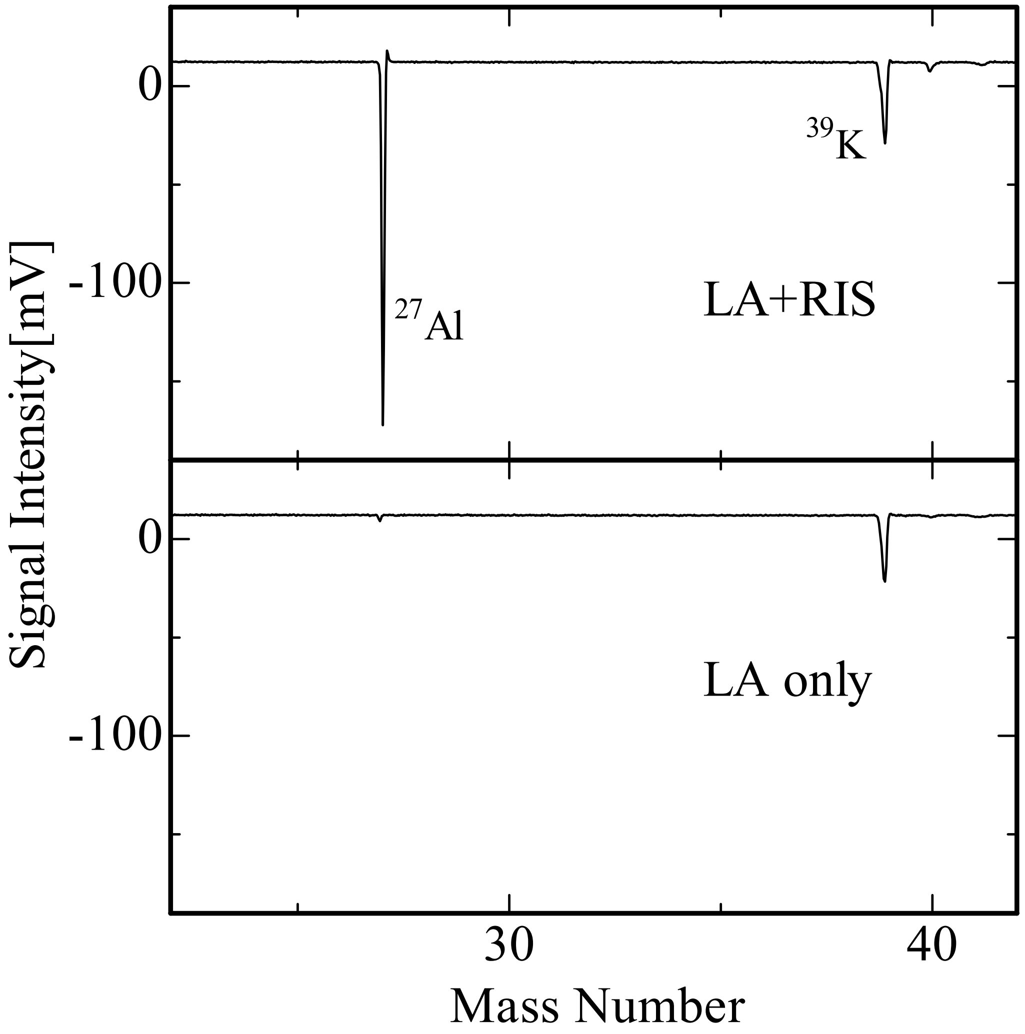

Fig. 4 K. Watanabe et al.

"Improvement of Resonant Laser Mass Spectrometry Using High-Repetition-Rate and Short-Pulse Tunable Laser System "

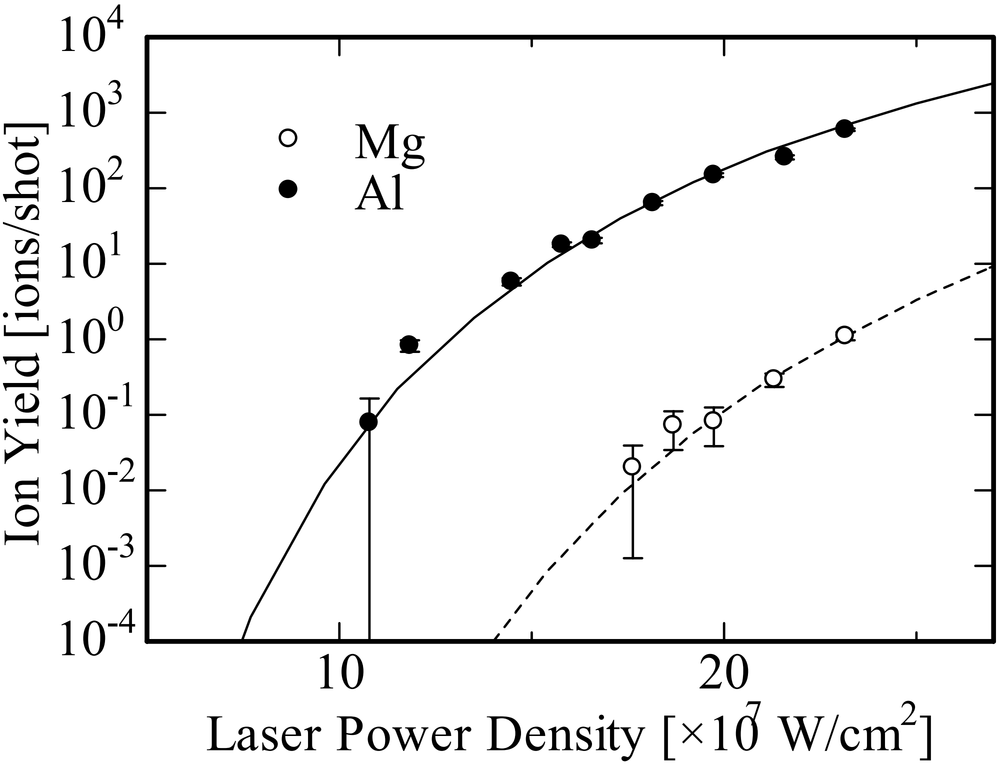

Fig. 5 K. Watanabe et al.

"Improvement of Resonant Laser Mass Spectrometry Using High-Repetition-Rate and Short-Pulse Tunable Laser System "

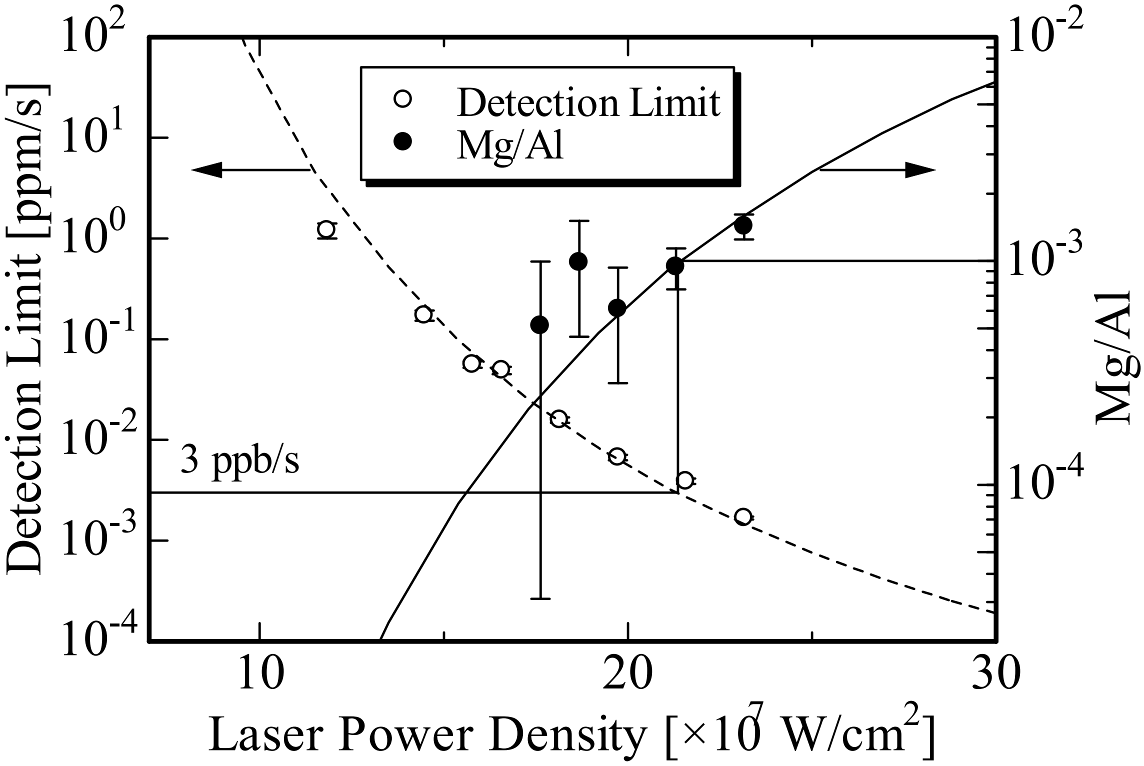

Fig. 6 K. Watanabe et al.

"Improvement of Resonant Laser Mass Spectrometry Using High-Repetition-Rate and Short-Pulse Tunable Laser System "

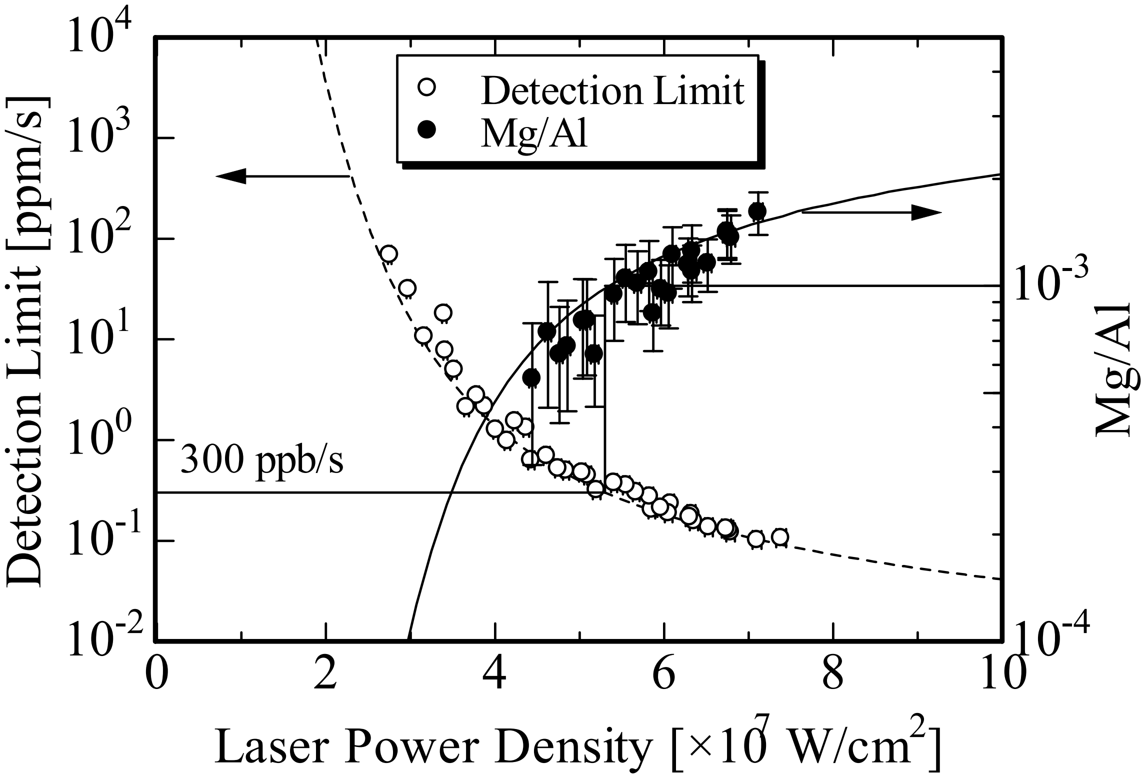

Fig. 7   K. Watanabe et al.

"Improvement of Resonant Laser Mass Spectrometry Using High-Repetition-Rate and Short-Pulse Tunable Laser System "

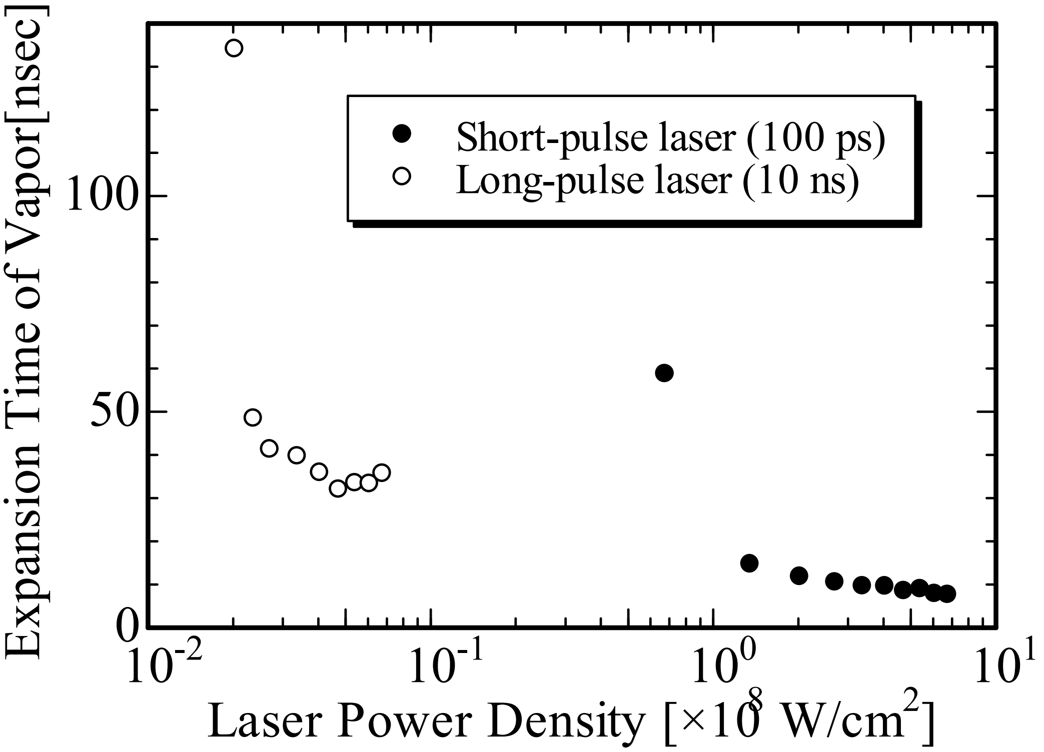

Fig. 8　K. Watanabe et al.

"Improvement of Resonant Laser Mass Spectrometry Using High-Repetition-Rate and Short-Pulse Tunable Laser System "